

# Partially deuterated poly(butadiene) Part II. Deuteron NMR investigation of strain-induced segment anisotropy

H. Menge\*, S. Hotopf, H. Schneider

*Universität Halle-Wittenberg, Fachbereich Physik, Friedemann-Bach-Platz 6, D-06108 Halle/Saale, Germany*

Received 15 March 1999; received in revised form 15 July 1999; accepted 2 September 1999

---

## Abstract

It is well known that deuteron NMR is a very sensitive tool for the investigation of order and orientation.  $^2\text{H}$  NMR measurements of partially deuterated poly(butadiene) elastomers with systematically varied elastic properties are presented.  $^2\text{H}$  NMR spectroscopy is applied to investigate the behaviour under uniaxially mechanical deformation. The segment order parameter  $S$  was found to be proportional to  $(\lambda^2 - \lambda^{-1})$ , but to be different for intercrosslinked chains and dangling ends. The line splitting for both components is indirectly proportional to the mean molar mass between crosslinks  $M_C$ . It is shown that the line splitting obtained from maxima position gives only information about more mobile parts of the network. The results are compared to  $^2\text{H}$  NMR transverse magnetization data based on the predictions of a model describing elastomer deuterium transverse magnetization data as a linear superposition of contributions from elastic chains and free dangling chain ends. The structural parameters are compared with results from mechanical and swelling measurements. The influence of microstructure, precursor chain length and their molar mass distribution as well as of the crosslink density on the transverse relaxation and the deformation behaviour were studied. © 2000 Elsevier Science Ltd. All rights reserved.

*Keywords:* NMR; Relaxation; Deformation

---

## 1. Introduction

Chemical characterization of elastomers is difficult because of the small amount of crosslinks present in these materials. However, the indirect observation of various crosslink densities through difference in molecular mobility has been reported recently in NMR relaxation [1–4] and imaging of elastomeric materials [5,6]. The transverse relaxation has shown to be the most sensitive to crosslinking. Transverse relaxation is mainly determined by dipole–dipole or quadrupolar interaction which is dramatically reduced by molecular motions for elastomers well above  $T_g$ . The observed residual interaction is due to rapid anisotropic segmental motion that is spatially inhibited by chemical crosslinks, topological chain constraints such as entanglements, or physical and chemical interactions acting as anchors for the rapid short-range processes [7–10]. Segment motions in undeformed elastomer average the  $^2\text{H}$  NMR spectrum to a single peak because of an isotropic distribution of end-to-end vectors, whereas the line shape is determined by the remaining quadrupolar interaction due

to this topological constrain. Mechanical deformation of elastomers preferentially orients the end-to-end vectors with respect to the strain axis. As a result, in uniaxially stretched rubber bands, the motional averaging of the quadrupole coupling is much more incomplete due to an additional strain-induced anisotropy, which results in a splitting of the isotropic signal into two peaks. Strain-induced orientation in mechanically deformed elastomers has received a lot of attention in recent years, in part due to the molecular level insights provided by  $^2\text{H}$  NMR investigation [11–17]. The segment anisotropy is characterized by an order parameter  $S$ , defined as

$$S = \langle P_2(\cos \psi) \rangle \quad (1)$$

where  $\psi$  is the angle between a segment vector and the strain axis and  $P_2(\cos \psi)$  is the second Legendre polynomial of  $\cos \psi$ ; the broken brackets represent the average over all segments. Classical elasticity theories predict a dependence of  $S$  on the deformation ratio  $\lambda$  ( $= l/l_0$ ) which is corroborated by experiments.

Many studies [17–19] was carried out on probe chains dissolved in uniaxially strained host networks. The induced alignment of the probe chains has been attributed to a nematic interaction between segments of the probe chain and elastomeric segments of the host network. However,

---

\*Corresponding author. Tel.: +49-345-55-25-595; fax: +49-345-55-27-161.

*E-mail address:* menge@physik.uni-halle.de (H. Menge).

Table 1  
Characterization of precursor poly(butadiene)

	Sample				
	A	B	C	D	E
$M_n$ (1,4-PB- $h_6$ )	120.000		125.000		61.000
$M_w$ (1,4-PB- $h_6$ )	450.000		129.000		64.000
$U$ (1,4-PB- $h_6$ )	3.75		1.03		1.05
$M_n$ (1,4-PB- $d_4$ )	190.000	152.000	135.000	70.000	50.000
$M_w$ (1,4-PB- $d_4$ )	700.000	162.000	140.000	72.000	52.000
$U$ (1,4-PB- $d_4$ )	3.68	1.06	1.05	1.03	1.04
Microstructure	97% <i>cis</i>	<i>cis/trans</i>	<i>cis/trans</i>	<i>cis/trans</i>	<i>cis/trans</i>

the order parameter of the probe chains is approximately equal to the order parameter of the host network, which is inconsistent with a nematic interaction. Recent experimental work was focused on the investigation of the relationship between the orientational anisotropy of dissolved chains and the elastic characteristics of host networks to resolve this inconsistency. Theoretical predictions [20,21] by Brereton and Ries suggest that the excluded volume interactions between segments subjected to the deformation cause anisotropic averaging of the quadrupolar interaction and thus cause a  $^2\text{H}$  NMR line splitting.

We present here the strain efficiency at inducing anisotropy, represented by the ratio  $S/(\lambda^2 - \lambda^{-1})$ , in random crosslinked partially deuterated poly(butadiene) elastomers which are varied in crosslink density, microstructure and precursor chain length/polydispersity. These networks are well characterized: mechanical properties, proton and deuteron NMR of the unconstrained samples have been reported previously [22,23].

On the other hand, it is well known that the mechanical properties of vulcanizates depend not only on the crosslink density, but also to a large extent on the vulcanization conditions such as curing agent, curing time and temperature [23,24]. The presence of a filler also contributes significantly to the mechanical properties. A deeper understanding of the mechanical properties of vulcanized elastomers may be gained from structural characterization of their networks. On the basis of the relationship between motional and structural parameters, an insight into the structural features of these materials should be available from those NMR parameters which are influenced by molecular mobility and order.

## 2. Experimental

All experiments were carried out on a Varian Unity 400 widebore spectrometer at 61.3 MHz for deuterons and at room temperature. Spectra were obtained using a standard  $90^\circ$  rf pulse of approximately  $7 \mu\text{s}$ . The deuteron measurements under mechanical deformation were performed by a simple stretching device parallel to the magnetic field. The stretching ratio  $\lambda$  ( $= l/l_0$ ) was determined from the distance

between two marks before and after stretching. The deconvolution of the spectra was performed using standard Varian software minimizing the difference between experimental and theoretical spectrum.

The elastomeric networks under study were based on partially  $\text{CD}_2$ -deuterated poly(butadiene) PB- $d_4$  with different microstructure, molar mass and mass distribution due to the polymerization process (see Table 1). They were mixed in a ratio 1:9 with a corresponding commercial poly(butadiene) with nearly the same parameters. Dicumyl peroxide was used as crosslinking agent in variable amount between 0.5 and 3 phr. The samples were vulcanized in a vulcameter press at  $145^\circ\text{C}$  and 100 bar for 1 h. The samples were characterized by mechanical and swelling measurements as well as by proton and deuteron transverse magnetization decay. From the magnetization decays the fractions of dangling ends, intercrosslink chains and the mean molar mass between two crosslinks  $M_C$  were determined using a two-component model described in detail in Refs. [1,5]. The results are published elsewhere [22,23].

## 3. Theory

### 3.1. $^2\text{H}$ spectroscopy under deformation

Deuteron NMR is very sensitive to strain-induced orientational anisotropy of polymer segments through the orientation-dependent quadrupolar interaction. The NMR frequency shift  $\Delta\nu_q$  caused by the quadrupolar interaction, reflects the time averaged orientation of a  $\text{C}-^2\text{H}$  bond:

$$\nu_q = \frac{3}{2} \delta_q \langle P_2(\cos \Theta(t)) \rangle \quad (2)$$

where  $\Theta$  is the orientation of a  $\text{C}-^2\text{H}$  bond with respect to the external magnetic field,  $P_2(\cos(\Theta(t)))$  is the second Legendre polynomial of  $\cos(\Theta(t))$ , and the brackets represent an average over the time of the NMR experiment.  $\delta_q$  ( $= e^2qQ/h$ ) is the static quadrupolar coupling, typically 164 kHz for an aliphatic bond ( $\delta_q = 4/3 \times \Delta\nu$  with a rigid lattice splitting of  $\Delta\nu = 123$  kHz). Eq. (2) assumes that the principal axis of the electrostatic field gradient is parallel to the  $\text{C}-^2\text{H}$  bond. The distribution of time-averaged  $\text{C}-^2\text{H}$  orientation in a sample is the distribution of quadrupolar frequencies and thus is the  $^2\text{H}$  NMR spectrum. Since the distribution of  $\text{C}-^2\text{H}$  orientation in deuterated elastomers is controlled by the distribution of polymer backbone segment orientations [25],  $^2\text{H}$  NMR spectra are interpreted as experimental measurements of elastomer-segment orientation distributions [11,24].

Segment motions in an undeformed elastomer are fast, but not isotropical due to the constraint produced by the crosslinking process [1,8]. Thus, they average the  $^2\text{H}$  NMR spectra to a single peak which is broader than in an un-crosslinked melt. A single peak is observed for an undeformed elastomer because there is an isotropic distribution

Table 2  
Network parameters (mean molar mass between crosslinks estimated from different methods, fractions)

Sample	Amount of DCP (phr)	$M_C$ (g/mol)					$^2\text{H}$ fraction of intercrosslinked chains A (%)	$^2\text{H}$ fraction of dangling ends B (%)	Free chains C (%)
			Mechanical	$^1\text{H}$ NMR (relaxation)	$^2\text{H}$ NMR (relaxation)	$^2\text{H}$ -NMR (Eq. (7))			
A-05	0.5	7590	8000	8200	8610	85.3	4.8	9.9	
A-08	0.8	5180	5000	4500	4510	87	7.6	5.4	
A-10	1	3230	4000	4260	4910	86	8.1	5.9	
A-12	1.2	2550	5300	5250	–	76.5	8.8	14.7	
A-15	1.5	3310	3400	3650	–	86	2.8	11.3	
A-20	2	2490	2200	1800	3550	89	3.1	7.7	
A-25	2.5	1330	1400	1150	–	87	4.2	8.8	
A-30	3	1060	1300	930	–	85	6.0	9.0	
B-05	0.506	–	10800	7240	3660	89	10.8		
C-05	0.55	3000	3040	5100	3500	91.8	7.9		
D-05	0.52	7200	5300	7760	7360	87.6	16.5		
E-05	0.635	5000	4700	6270	7240	78	21.5		

of end-to-end vectors [24]. Mechanical deformation of elastomers preferentially orients the end-to-end vectors with respect to the strain axis which is parallel to the static magnetic field  $B_0$  in our case. As a result the motional averaging of the quadrupolar interaction is additional anisotropic due to the applied force, and the experimentally observed  $^2\text{H}$  NMR spectrum splits into two peaks. The  $^2\text{H}$  NMR spectral splitting  $\Delta\nu$ , induced by uniaxial strain may be predicted by averaging Eq. (2) over all C– $^2\text{H}$  bond orientations compatible with the end-to-end vectors that are preferentially oriented relative to the strain axis [11]. This averaging leads to an expression for  $\Delta\nu$  that depends on the angle between the strain axis and the external magnetic field direction. In a lot of previous papers, for an elastomer strained along an axis parallel to the external magnetic field the splitting was given by

$$\Delta\nu = \frac{3}{2} \delta_q \langle P_2(\cos \phi) \rangle \langle P_2(\cos \psi) \rangle \quad (3)$$

where  $\phi$  is the angle between a C– $^2\text{H}$  bond and the vector of the segment to which it is attached and  $\psi$  is the angle between the segment vector and the strain axis. Based on different theoretical attempts to simultaneously explain the line broadening and the quadrupolar splitting of the  $^2\text{H}$  NMR spectra developed independently by Sotta/Delocche [13] and Brereton/Ries [21] this result seems to be incorrect, because in Eq. (3) only the deformation of the end-to-end vector is considered which does not result in a splitting due to their calculations. To obtain splittings one needs interaction (nematic coupling or excluded volume potential) which should result in an additional factor in Eq. (3) reflecting the strength of this interaction. Nevertheless, because  $\langle P_2(\cos \psi) \rangle$  is the segment order parameter  $S$ , Eq. (3) states that the  $^2\text{H}$  NMR spectral splitting  $\Delta\nu$  is directly proportional to the segment order parameter for an elastomer under uniaxial strain which is consistent with the experimental observation.

The earliest theoretical description of the segment order

parameter  $S$  is given by Kuhn and Gr $\ddot{u}$  n [25]. They calculated the average orientation of the statistical chain segment in perfectly elastic networks. Their analysis combined with the assumption of an affine deformation predicts that the order parameter  $S$  is inversely proportional to the average number of segments  $N_s$  in the intercrosslink chain:

$$S = \frac{1}{5N_s} \left( \lambda^2 - \frac{1}{\lambda} \right) \quad (4)$$

With  $\langle P_2(\cos \phi) \rangle = -0.154$  (determined by simulation [11] of a poly(butadiene) chain with 50% *cis*- and *trans*-1,4 units, respectively) Eq. (3) can be simplified, giving

$$\Delta\nu = \frac{3}{2} \delta_q 0.154 S \quad (5)$$

## 4. Results and discussion

### 4.1. Characterization of the undeformed networks

Number-average molecular weights between crosslinks  $M_C$  of the randomly crosslinked partially CD $_2$ -deuterated poly(butadiene)-d $_4$  networks were obtained from transverse NMR relaxation and mechanical measurements (Table 2). Additionally, the weight fraction of intercrosslink chains and dangling ends were determined from proton and deuteron transverse NMR relaxation. These magnetization decays can be represented as a sum of two components: one contributed from segments in elastic, intercrosslinked chains,  $M_{\text{NW}}(t)$ , and the other contributed from segments in dangling or pendant chains,  $M_{\text{DE}}(t)$ :

$$\frac{M(t)}{M(0)} = A \times M_{\text{NW}}(t) + B \times M_{\text{DE}}(t) \quad (6)$$

The components are distinguished by shape and dephasing rate, due to differences in segmental mobility between intercrosslinked chains A and dangling ends B. Segments in

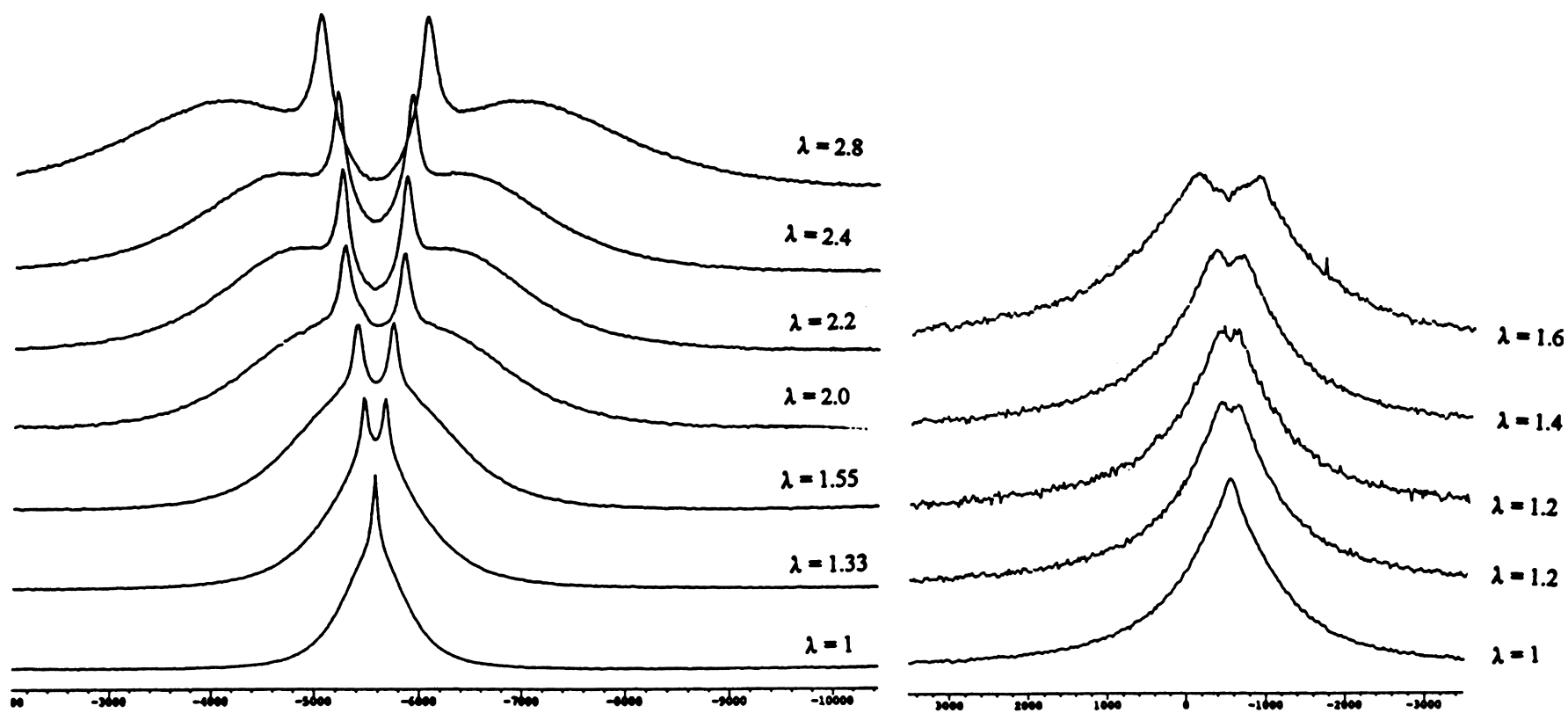


Fig. 1.  $^2\text{H}$  NMR spectra deuterated *cis*-poly(butadiene) networks at different uniaxial deformation ratios: left—sample A-05; right—sample A-30.

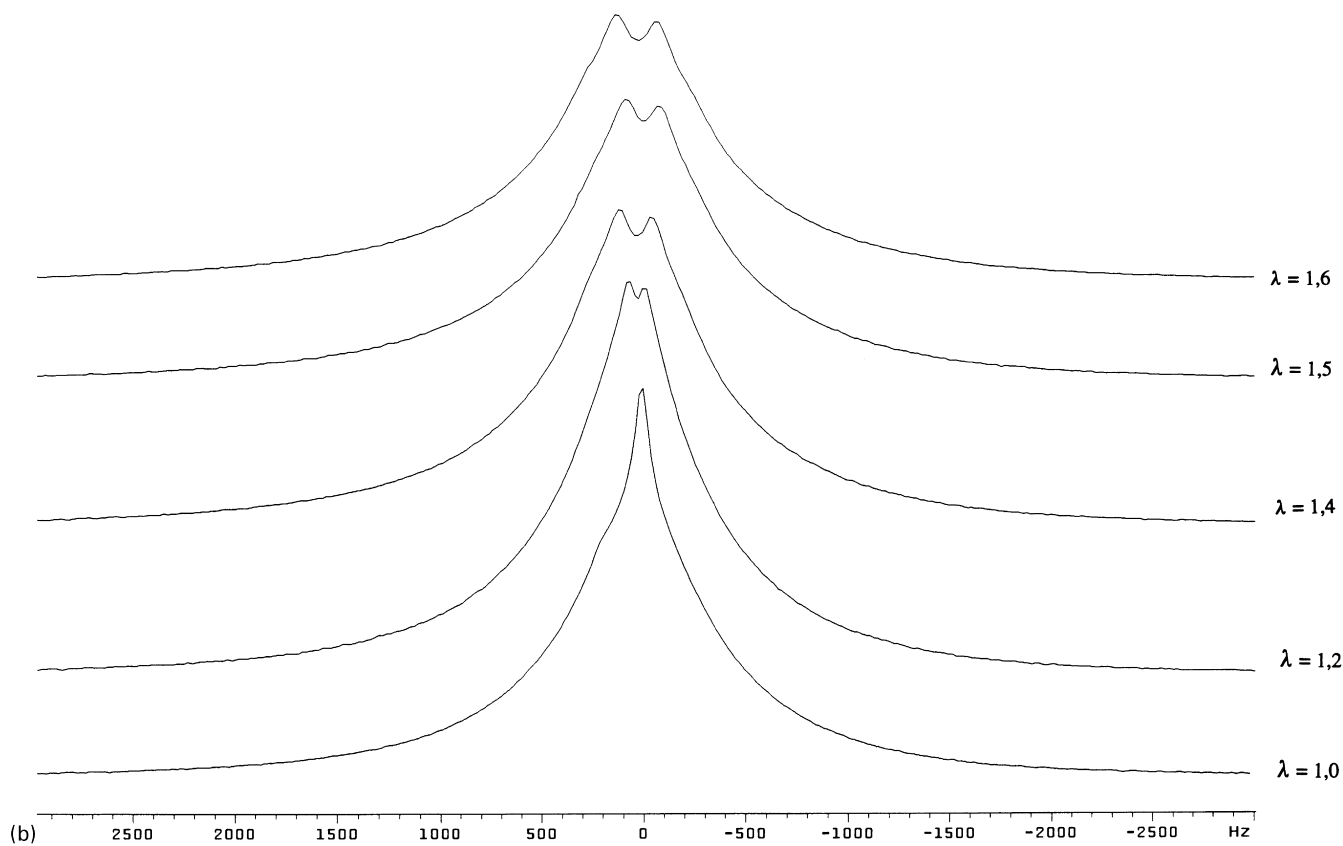
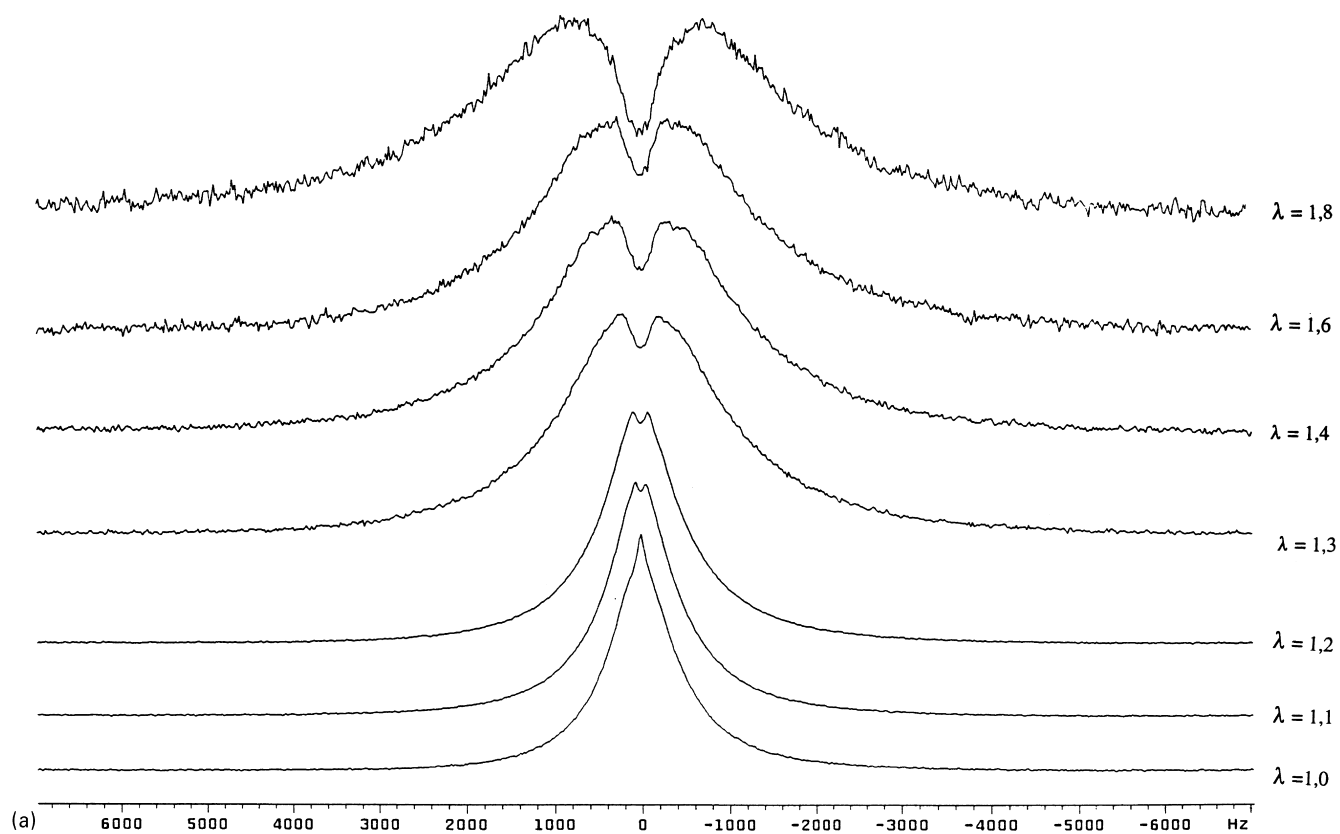


Fig. 2.  $^2\text{H}$  NMR spectra deuterated *cis/trans*-poly(butadiene) networks prepared from long (a) and short (b) precursor chains at different uniaxial deformation ratios: (a) B-05; (b) D-05.

dangling ends can reorient isotropically on NMR scale, but intercrosslinked chains reorient anisotropically, due to topological constraints like crosslinks. As a result, the contribution of the dangling ends  $M_{DE}(t)$  can be represented by an exponential decay with a relaxation time  $T_2$  corresponding to rapid motional averaging. The contribution from intercrosslinked chains is here described by an expression given by Simon et al. [1] for anisotropic motional averaging. Alternatively, an expression developed by Sotta et al. [7] can be used. The results concerning the crosslink density are equivalent, however, the fraction of dangling ends is neglected there.

#### 4.2. Dependence of strain-induced anisotropy in partially deuterated butadiene rubber

The number-average molecular weights, polydispersities and microstructure of polymer precursor obtained by GPC measurements are indicated in Table 1.

The strain dependence of  $^2\text{H}$  NMR spectral splitting observed for a set of random crosslinked  $\text{CD}_2$ -deuterated butadiene rubber network stressed along an axis parallel to the external magnetic field  $B_0$  for two different crosslink densities of sample series A is shown in Fig. 1 and for different precursor chain length and microstructure, but same amount of crosslinker (series B and D) in Fig. 2(a) and (b). The line splitting observed in the  $^2\text{H}$  NMR spectra of deformed networks increases with larger crosslink density. The longer the length of the precursor chains the larger the line splitting at the same deformation ratio and at approximately the same crosslink density. The length of the precursor chain also affects the line width and the fraction of defects like dangling ends: a shorter precursor narrows the line and increases the amount of defects.

The deformation dependence of sample A-05 (high-*cis* microstructure, 0.5 phr DCP) clearly shows two separated doublets at larger deformation ratios (Fig. 1). All spectra of sample series A independent on their crosslink density can be deconvoluted into two sets of Lorentzian lines at all deformations (in the following called “inner” and “outer” splitting). The  $^2\text{H}$  NMR spectra of the nondeformed network can be represented by a superposition of only two Lorentzian lines, which represent contributions from intercrosslink chains and from dangling ends (including also a small amount of some free, soluble chains) as proposed by several authors [1,18,19,26]. To test this assumption, the behaviour of the individual peaks (found by deconvolution) of the  $^2\text{H}$  NMR spectra was considered. It is clearly shown in Figs. 3 and 4 that the linewidth of the two distinct contributions shows a different dependence on the crosslinking density and on the deformation ratio: while the linewidth of the “inner” splitting does nearly not change, the linewidth of the “outer” splitting shows a large broadening with increasing amount of crosslinker as well as further stretching.

The splittings  $\Delta\nu$  of both contributions are plotted as a linear function of  $(\lambda^2 - \lambda^{-1})$ , and they are well-presented by straight lines through the origin (Fig. 5). However, their slopes are different. The “outer” splitting increases much faster than the “inner” splitting. In comparison with the results from the relaxation measurements [22,23] and also due to the range of splitting and the linewidth (the “inner” splitting shows substantially narrower lines than the “outer” one), these two different splittings could be attributed to the contributions from the intercrosslink chains (“outer” splitting) and the sum of dangling ends and a small amount of free chains (“inner” splitting). The same deconvolution could be performed to sample series B–E with an additional set of Lorentzian lines for *trans* configuration.

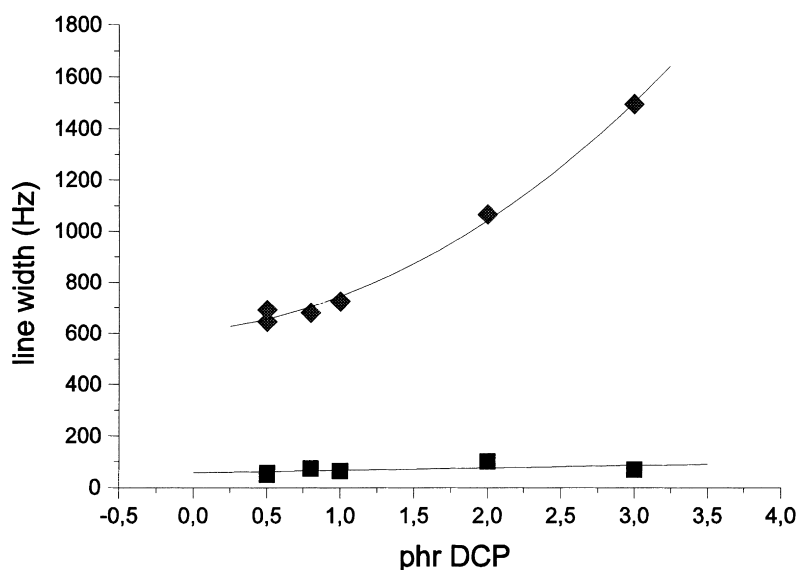


Fig. 3.  $^2\text{H}$  NMR linewidth of the two different contributions (from superposition of two NMR lines) for the non-stretched *cis*-polymer network A vs. amount of crosslinker DCP: (■) narrow line due to pendant chains; (◆) broad line due to intercrosslinked chains.

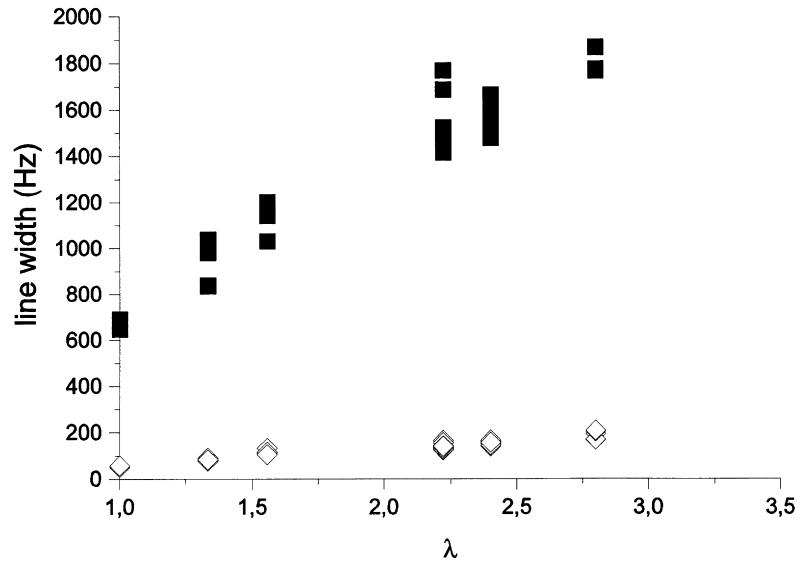


Fig. 4. <sup>2</sup>H NMR linewidth of the two different contributions (from superposition of two NMR lines) for the non-stretched *cis*-polymer network A-05 vs. deformation ratio: (◇) narrow line due to pendant/free chains; (■) broad line due to intercrosslinked chains.

As already reported by Gronski et al. [11] the *cis* and the *trans* configuration show different splittings by an order of 2. However, there were some problems to find a really good fit due to the low possible deformation ratio of the sample series B–E prepared by anionic polymerization. The result of deconvolution is shown in Fig. 6. The slopes  $\Delta\nu/(\lambda^2 - \lambda^{-1})$  of all different contributions (determined from best linear fit) are proportional to  $1/M_C$  and represent the strain efficiency. The dependence of the slopes on the mean molecular weight between two crosslinks (number average) is shown in Fig. 7 for all three components (*cis*- and *trans*-intercrosslink chain, sum of dangling ends and free chains). The data could be represented by separated straight lines for

the *cis*-network component and for the more mobile chains (dangling ends, free chains), indicating different strain efficiencies of both portions. The slope of the *trans*-configuration seems to differ, but this could probably be caused by the above-mentioned fit uncertainty. So far, from the linear dependence of splitting on the deformation the behaviour seems to be affine. However, data from recently performed SANS measurements could be well described in terms of a nonaffine tube diameter deformation [27,28]. So further focus will be directed on the shape of those lines attributed to intercrosslinked chains.

If the above supposed resulting additional factor  $f(U)$  describing the strength of the coupling interaction is in the

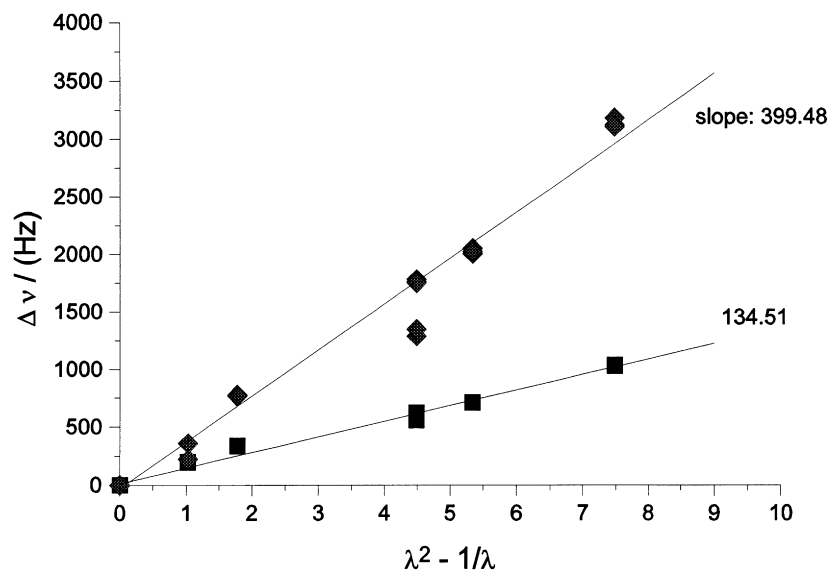


Fig. 5. Dependence of the <sup>2</sup>H NMR spectral splittings,  $\Delta\nu$ , of the two different components (from deconvolution) on  $(\lambda^2 - \lambda^{-1})$  for the *cis*-polymer network A-05: (■) narrow line due to pendant chains; (◆) broad line due to intercrosslinked chains.

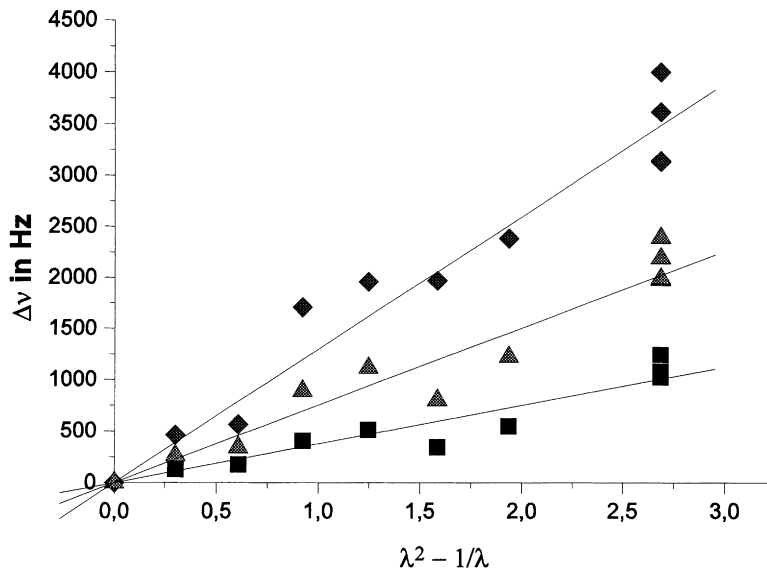


Fig. 6. Dependence of the  $^2\text{H}$  NMR spectral splittings,  $\Delta\nu$ , of the two different components (from deconvolution) on  $(\lambda^2 - \lambda^{-1})$  for the *cis/trans*-network B-05: (■) narrow line due to pendant chains; (▲) broad line due to intercrosslinked chains in *cis* configuration; and (◆) broad line due to intercrosslinked chains in *trans* configuration.

order of 1 it should be possible by using Eqs. (3) and (4) to approximate roughly the mean molecular mass between two crosslinks from the splitting of the network chains (“outer” splitting) via the number of statistical segments  $N_s$ :

$$N_s = \frac{2}{5} \frac{\Delta f}{\Delta \nu} \left( \lambda^2 - \frac{1}{\lambda} \right) f(U) \quad (7)$$

The mass of a statistical segment of poly(butadiene) is about 70 g/mol (dependent on the microstructure) given by Aharoni [29,30]. The agreement compared with the results from  $^1\text{H}$ ,  $^2\text{H}$  NMR relaxation, stress–strain and swelling

measurements is in most cases very well within an error limit of about  $\pm 15\%$  (see Table 2). The discrepancies arise with the smaller available deformation range. The fractions of elastic chains A and pendant chains B ( $= 1 - A$ ) found here are comparable to those from the relaxation measurements [22,23].

In a lot of previous papers the splitting was simply obtained from peak maxima [11–17,19,26,31] of the doublets. Compared with our data these peak maxima are mainly determined by dangling ends and free chains and correspond to an order parameter of those chains. This is in agreement

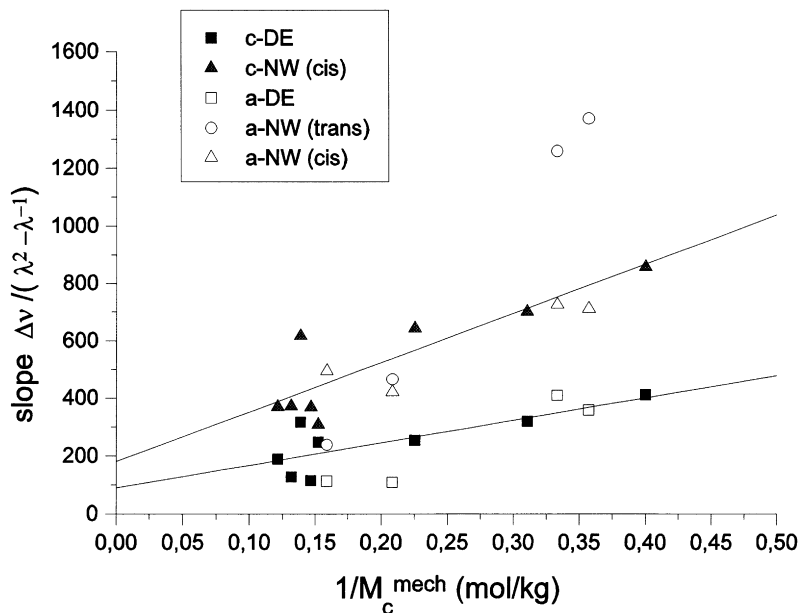


Fig. 7. Dependence of  $\Delta\nu(\lambda^2 - \lambda^{-1})$  on the molecular weight between crosslinks  $M_c$  for the narrow and broad lines, respectively, for all networks under study (abbreviations: DE—dangling ends; NW—network; c—sample series A; a—sample series B–E).



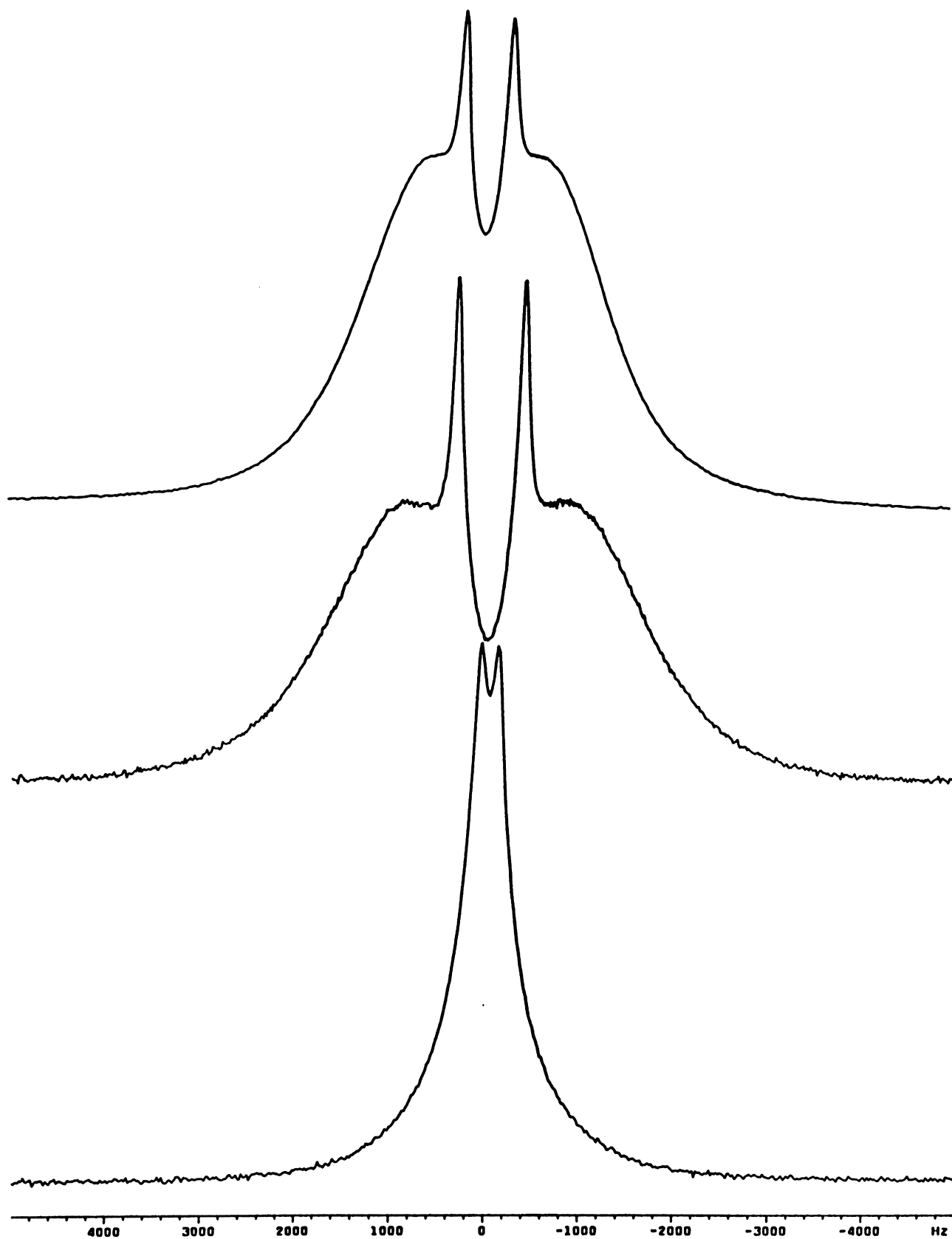


Fig. 8. Comparison of the  $^2\text{H}$  NMR spectra obtained from network A-05 (10% PB- $d_4$ ) and A-05-2 (20% PB- $d_4$ ): bottom:  $^2\text{H}$  NMR spectra from A-05-2 at  $\lambda = 2.5$  before extraction; middle:  $^2\text{H}$  NMR spectra from A-05 at  $\lambda = 2.54$ ; top:  $^2\text{H}$  NMR spectra from A-05-2 at  $\lambda = 2.0$  after extraction in toluene.

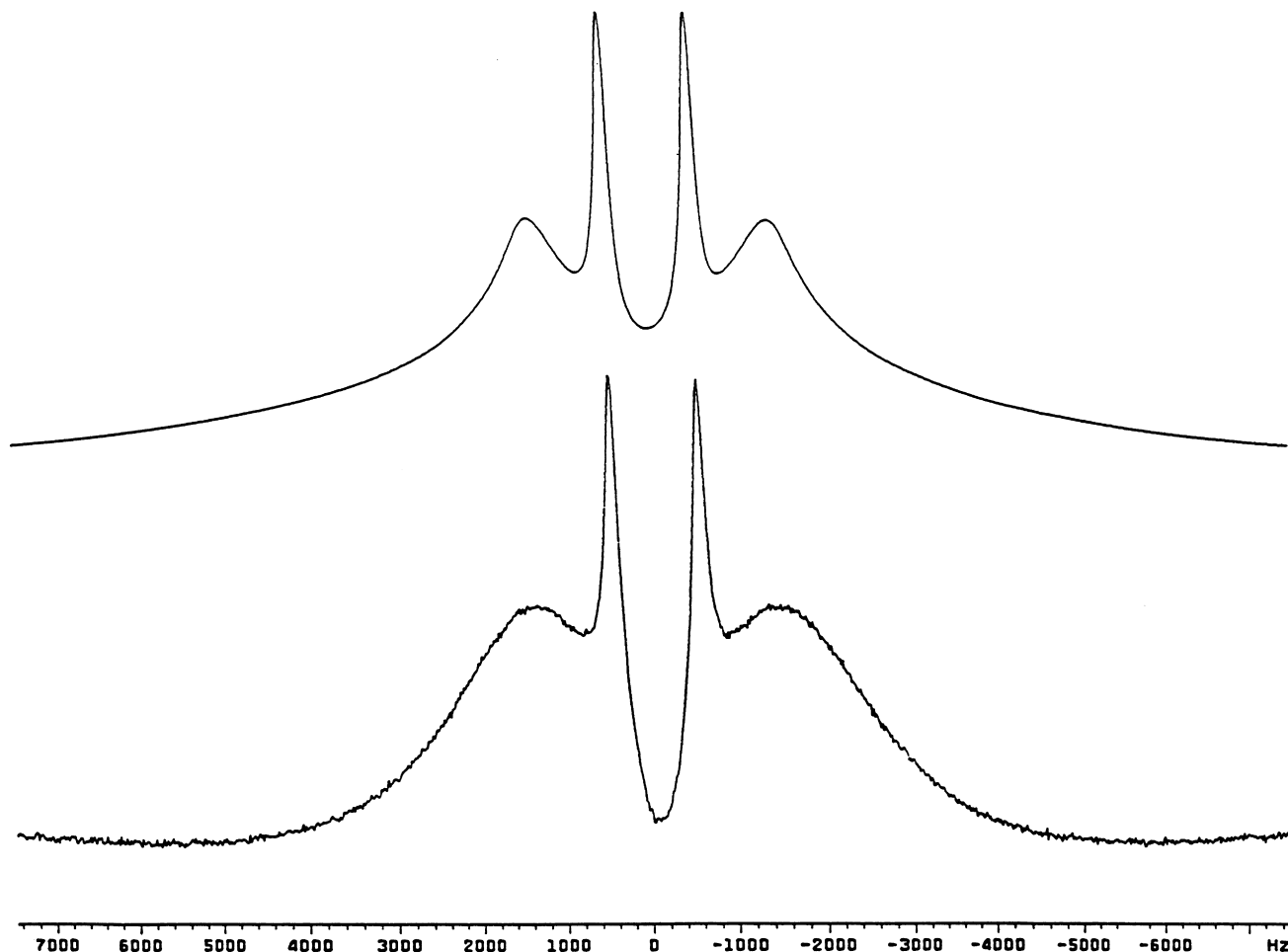


Fig. 9. Comparison between experimental and simulated  $^2\text{H}$  NMR spectra for network A-05 at  $\lambda = 2.8$ . The simulation based on the model proposed by Sotta and Deloche (Eqs. (8) and (9)) with the assumption of a superposition of the contributions from intercrosslinked chains and dangling ends. The parameters  $N_{\text{NW}} = 90\text{--}100$ ,  $A = 0.85$ ,  $N_{\text{DE}} = 290$ ,  $B = 0.15$ ,  $T_2^{\text{NW}} = 5$  ms,  $T_2^{\text{DE}} = 10$  ms,  $\lambda = 2.8$  and an adjustable, but unique value  $U/5$  in the order of  $10^{-1}$  were used. The mass of the statistical segment of poly(butadiene) was 70 g/mol given by Aharoni.

with an explanation of Kornfield et al. [26] suggesting that the central portions of  $^2\text{H}$  NMR spectra of elastomers are dominated by deuterons in pendant chains. To test this suggestion, already Mc Loughlin et al. [18,19] prepared elastomers with deuterium labelling only in pendant chains by endlinking mixtures of deuterated monofunctional chains and nondeuterated difunctional chains. However, within the error limits they did not find any difference for compressed, randomly deuterated networks and splittings for segments in pendant chains attached to the compressed networks. They concluded that this was not a proof or disproof of the suggestion by Kornfield et al. [26] because the splittings reported for the randomly deuterated networks were obtained from peak maxima which may correspond to pendant-chain contributions to the  $^2\text{H}$  NMR spectra.

This latter argument may also be supported by the interpretation and comparison of the two samples A-05 and A-05-2. Both samples were prepared on the basis of exactly the same precursor polymer and the same amount of crosslinker Dicumyl peroxide DCP (0.5 phr DCP). The preparation and

vulcanization process was identical with the exception of a higher portion of partially deuterated chains PB-d<sub>4</sub> (mixing ratio of sample A-05-2 was 2:8 instead of 1:9). Thus, the  $^2\text{H}$  NMR spectra of the two samples were expected to be identical. However, they differ in line shape and splitting as it is shown in Fig. 8(a) and (b) at approximately the same deformation ratio. Performing and analysing the transverse relaxation measurements as well as for protons as for deuterons (as described in [1,5,22]), the portions of intercrosslinked chains, of free dangling ends, of free, soluble chains and the mean molar mass between crosslinks  $M_C$  were determined. A larger portion of dangling ends and free chains ("sol"-content) were obtained in the sample A-05-2 compared to A-05. The extraction procedure of the network sample A-05-2 in toluene ended with a mass loss of about 40%. The  $^2\text{H}$  NMR spectra after extraction were the expected ones (Fig. 8(c)). The investigation of the extracted solution by infrared spectroscopy and GPC indicates a mixture of deuterated and protonated polymer corresponding to the initial mixing ratio and a number average

molar mass  $M_n$  of 49 000 g/mol and a weight average  $M_w$  of 213 000 g/mol. The width of the molecular mass distribution was found to be similar to that of the precursor mass distribution, but shifted towards shorter chains. These shorter removable chains are responsible for the much narrower lines and the smaller observed peak-to-peak splitting. The reduction of the contribution from the free chains was also checked by relaxation measurements. The  $M_C$  values of both samples determined from transversal relaxation were nearly the same as expected and remain unchanged due to the extraction procedure.

Sotta and Deloche [13] and also Brereton [20,21] had pointed out that a segment interaction is necessary to obtain not only differences in the line shape but also a line splitting in the  $^2\text{H}$  NMR spectra at a certain deformation. The difference between both approaches consists in the kind of description of these interactions. Sotta and Deloche [13] assumed it to be a nematic one. In their paper [13] they give an expression of the residual quadrupolar interaction  $\Delta_R$  in deformed elastomer networks ( $\alpha$  is the angle of the end-to-end vector  $\mathbf{R}$  with respect to  $B_0$  and  $\Omega$  is the angle between  $B_0$  and the stress direction):

$$\Delta_R = \nu_q \left[ \frac{3}{5} \left( \frac{r^2}{N} \right) P_2(\cos \alpha) + \frac{U}{5} S P_2(\cos \Omega) \right] \quad (8)$$

$$\text{with } S = \left[ \frac{1}{5-U} \right] \left( \frac{\sigma^{-2}}{N} \right) \left( \lambda^2 - \frac{1}{\lambda} \right)$$

Here  $r = \mathbf{R}/\mathbf{R}_0$  is the ratio of end-to-end vector  $\mathbf{R}$  to the root-mean-square end-to-end vector of the corresponding chain in the melt (ideal chain)  $\mathbf{R}_0 = N^{1/2}a$ , where  $N$  is the number of segments in the chain and  $a$  is their length. The distribution of end-to-end vectors are assumed to be Gaussian in their calculations. For Gaussian chains,  $\sigma^2$  equals  $3/2$ .  $S$  is the order parameter and the parameter  $U$  characterizes the segmental interaction strength (in  $k_B T$  units). From comparison with the experimental spectrum Sotta et al. found an adjustable value  $U/5$  of the order of  $10^{-1}$ .

Using the information from the transversal relaxation about the number of segments  $N_{\text{NW}}$  between two crosslinks and the number of segments  $N_{\text{DE}}$  in a dangling end, the fractions of intercrosslink chains A, the fraction of the dangling ends B ( $= 1 - A$ ) and their relaxation times  $T_2$ , the  $^2\text{H}$  NMR spectra can be simulated as a superposition from these two contributions (Fig. 9). The assumptions are only that both kinds of chains experience the same segment interaction strength  $U$ , but the dangling ends feel only the second term of Eq. (8) and can be of different length  $N_{\text{DE}}$ , whereas the intercrosslinked chains are stressed to a new end-to-end vector (responsible for the line broadening). The  $^2\text{H}$  NMR spectra were obtained by Fourier transformation of the relaxation function [13]  $M(t)$  with the above mentioned modifications (where the stress direction is parallel to

magnetic field ( $\Omega = 0^\circ$ )

$$M(t) = M_0 \left[ A \int h_\lambda(\mathbf{R}) d\mathbf{R} \exp(-t/T_2^{\text{NW}}) \cos(\Delta_R t) + B \int h_{\text{is}}(\mathbf{R}) d\mathbf{R} \exp(-t/T_2^{\text{DE}}) \cos\left(\nu_q \frac{U}{5} S t\right) \right] \quad (9)$$

The spatial integration element,  $d\mathbf{R}$ , is  $r^2 dr d\omega$ . When the external force  $\mathbf{F}$  is applied, the end-to-end vectors are assumed to deform affinely, the volume element remains constant; thus for an elongation  $\lambda$ , the isotropic distribution [13]  $h_{\text{is}}(\mathbf{R}) = 4\sigma^3 \pi^{1/2} \exp(-\sigma^2 r^2)$  becomes  $h_\lambda(\mathbf{R}) = 4\sigma^3 \pi^{1/2} \exp[-(\sigma^2 r^2/\lambda^2)[\lambda^3 - (\lambda^3 - 1) \cos^2 \chi]]$  where  $\chi$  is the angle between  $\mathbf{R}$  and  $\mathbf{F}$  (see also [13]).

So the two experimentally found doublets can be used to fix the segmental interaction strength  $U$  ( $U \approx 0.5$ ) which is near to the orientational coupling strength of poly(butadiene)  $\epsilon = 0.4$  given by infrared-dichroism and birefringence [32]. Fig. 9 shows that the peak position is well represented. The line width of the peak attributed to the pendant chains is similar to the experimental one, but the shape of the broad line differs.

So far, the results are also consistent with predictions of a recent theoretical study by Brereton and Ries [20,21]. The authors showed that the line splitting can be accounted for by considering the effect of isotropic excluded volume interactions rather than a nematic interaction between the segments. From theoretical point of view, their analysis encompasses the more general case of dissolved probe chains with a chemical structure different from the host. The results of McLoughlin et al. [18,19] from the comparison of the splittings measured in PDMS host networks and dissolved probe chains seem to support this theoretical analysis, however the splittings for the host network were obtained from peak maxima which may correspond to pendant chain contribution to the  $^2\text{H}$  NMR spectra. Brereton and Ries [20,21] also considered the effect of molecular weight of the probe chains relative to  $M_C$ . They found that the line splitting  $\Delta\nu_{\text{A/B}}$  from either the network or free chains can be written as

$$2\pi\Delta\nu_{\text{A/B}} = 2(\lambda^2 - \lambda^{-1})\Delta_{\text{A/B}}(\chi_F, N_A, N_B, c_A, c_B) \quad (10)$$

with

$$\Delta_{\text{A/B}} = \frac{2}{15\pi} \frac{1}{cb^3} \frac{\nu_0}{N_A} \frac{c_A}{c} \left[ \frac{b}{\xi} + \frac{c_B}{c} F_{\text{A/B}}(\chi_F, N_A, N_B, c_A, c_B) \right] \quad (11)$$

The deformation dependence is entirely contained in the prefactor of Eq. (10), whereas the molecular weight, concentration and temperature dependences are contained in the term  $\Delta_{\text{A/B}}$  (Eq. (11)), where  $F_{\text{A/B}}$  are explained in detail in the original paper [20,21],  $b$  is the average segment length,  $c$  ( $c = c_A + c_B$ ) is the total segment concentration such that  $cb^3 = 1$  in the absence of small-molecule solvents.  $N_{\text{A/B}}$  represents either the number of segments  $N_A$  of an

elastic chain or the number of segments  $N_B$  of a dissolved probe chain.  $\nu_0$  is the  $^2\text{H}$  interaction constant and  $\xi$  the Edwards screening length.

With the assumption of a fast dynamics for polymer chains, for free chains this leads to narrow lines independent of the deformation. However, for the network chains there is a contribution to the line shape which comes from the constraint on the end-to-end vector. Assuming that an elastic (intercrosslink) chain is stretched under deformation to a new end-to-end length, the number of conformations which are allowed is restricted (and therefore also the mobility of the chains is reduced), the spectra should broaden. For both network and free chains the splitting is inversely proportional to  $N_A$ , the molecular weight between crosslinks, as we found experimentally.

In the case that the chains (network as well as dissolved chains) are chemical identical but of different molecular weights they predict due to the first term of Eq. (10) a linear dependence on the network fraction  $c_A$ . However, in this case, they give an expression for  $F_{A/B}$  ( $\chi_F = 0, N_A, N_B, c_A, c_B$ ) which is *the same for both kinds of chains*. A more detailed study and discussion to solve this contradiction to our experimental results is in progress. Based on the results of Bates [33], we do not expect an influence of any  $\chi$  parameter due to the mixing ratio of protonated and deuterated poly(butadiene) chains to explain our experimental results. The argument to produce a very inhomogeneous network with this kind of crosslinker (which could explain the two splittings at larger deformation ratios) we can exclude based on results of SANS measurements under strain [27,28].

## 5. Conclusion

Segment order parameter,  $S$ , measured by  $^2\text{H}$  NMR for uniaxially stretched randomly crosslinked partially deuterated poly(butadiene) elastomers depend linearly on  $\lambda^2 - \lambda^{-1}$ , where  $\lambda$  is the deformation ratio. The line splitting observed in the  $^2\text{H}$  NMR spectra of deformed networks increases with larger crosslink density. The longer the length of the precursor chains the larger the line splitting at the same deformation ratio and at approximately the same crosslink density. The length of the precursor chain mainly affects the line width and the fraction of defects like pendant chains. For all samples and deformation ratios, independent on microstructure and precursor, the  $^2\text{H}$  NMR spectra could be deconvoluted into two contributions arising from elastic, intercrosslinked chains (depending on the microstructure either only *cis*- or both *cis*- and *trans*-configuration) and from pendant chains. While the dangling ends show narrow lines, the network chains broaden very strongly with stretching. The strain efficiency  $\Delta\nu/(\lambda^2 - \lambda^{-1})$  for all components (intercrosslink chains; free dangling ends) was found to be proportional to  $1/M_C$ , but differs from each other. We have shown that the usual used splitting determined from the

doublet maxima is dominated by pendant and free chain contributions. The resulting crosslink densities agree well with those from transverse relaxation measurements and mechanical module dependencies.

## Acknowledgements

S.H. acknowledges the Deutsche Forschungsgemeinschaft (DFG) (project: Schn 407/2-1,2-2) and the Sonderforschungsbereich SFB 418 for financial support. The authors thank Dr Wim Pyckhout-Hintzen and Ms Marlies Hintzen both from IFF at FZ Jülich for their support concerning laboratory capacity for sample preparation and chemical characterization. H.M. thanks additionally Dr Wim Pyckhout-Hintzen and Dr Gerd Meier (MPI for polymer research in Mainz) for their help to perform SANS measurements.

## References

- [1] Simon G, Gronski W, Baumann K. *Macromolecules* 1992;25:3624 and references therein.
- [2] Gronski W, Hoffmann U, Simon G, Wutzler A, Straube E. *Rubber Chem Technol* 1992;65:63.
- [3] Fülber C, Demco DE, Weintraub O, Blümich B. *Macromol Chem Phys* 1996;197:581.
- [4] Malveau C, Tekely P, Canet D. *Solid State Nucl Magn Reson* 1997;7:271.
- [5] Kuhn W, Barth P, Hafner S, Simon G, Schneider H. *Macromolecules* 1994;27:5773.
- [6] Knörger M, Heuert U, Schneider H, Barth P, Kuhn W. *Polym Bull* 1997;38:101.
- [7] Sotta P, Fülber C, Demco DE, Blümich B, Spiess HW. *Macromolecules* 1996;29:6222.
- [8] Cohen-Addad JP. NMR and fractal properties of polymeric liquids and gels. In: Emsley JW, Feeney J, Sutcliffe LH, editors. *Progress in NMR spectroscopy*, Oxford, UK: Pergamon Press, 1993 and references therein.
- [9] Simon G, Götschmann B, Matzen D, Schneider H. *Polym Bull* 1989;21:475.
- [10] Lee S, Pawlowski H, Coran AY. *Rubber Chem Technol* 1994;67:854.
- [11] Gronski W, Stadler R, Jacobi MM. *Macromolecules* 1984;17:741.
- [12] Deloche B, Beltzung M, Herz J. *J Phys (Paris) Lett* 1982;43:763.
- [13] Sotta P, Deloche B. *Macromolecules* 1990;23:1999.
- [14] Deloche B. *Makromol Chem, Macromol Symp* 1993;72:29.
- [15] Chapellier B, Deloche B, Oeser R. *J Phys II France* 1993;3:1619.
- [16] Jacobi MM, Abetz V, Stadler R, Gronski W. *Polymer* 1996;37:1669.
- [17] Simon G. *Polym Bull* 1991;25:365.
- [18] McLoughlin K, Szeto C, Duncan TM, Cohen C. *Macromolecules* 1996;29:5475.
- [19] McLoughlin K, Waldbieser JK, Cohen C, Duncan TM. *Macromolecules* 1997;30:1044.
- [20] Brereton MG. *Macromolecules* 1993;26:1152.
- [21] Brereton MG, Ries ME. *Macromolecules* 1996;29:2644.
- [22] Menge H, Hotopf S, Schneider H, Heuert U. *Polymer* 1999 in press.
- [23] Hotopf S, Menge H, Schneider H. In: te Nijenhuis K, Mijis WJ, editors. *The Wiley polymer network review*, 1. New York: Wiley, 1998 Papers from the Polymer Networks Group International Conference 1996, Delft, Netherlands.
- [24] Mark JE, Erman B. *Rubberlike elasticity: a molecular primer*, New York: Wiley-Interscience, 1988.
- [25] Kuhn W, Grün F. *Kolloid Z* 1942;101:248.

- [26] Kornfield JA, Chung G-Ch, Smith StD. *Macromolecules* 1992;25:4442.
- [27] Straube E, Urban V, Pyckhout-Hintzen W, Richter D, Glinka CJ. *Phys Rev Lett* 1995;74:4464.
- [28] Menge H, Pyckhout-Hintzen W, Straube E, Meier G, Hotopf S. In preparation.
- [29] Aharoni SM. *Macromolecules* 1983;16:1722.
- [30] Aharoni SM. *Macromolecules* 1986;19:426.
- [31] Poon C, Samulski E, Nakatani A. *Makromol Chem, Makromol Symp* 1990;40:109.
- [32] Ylitalo CM, Fuller GG, Abetz V, Stadler R, Pearson DS. *Rheol Acta* 1990;29:543.
- [33] Bates FS, Wiltzius P. *J Chem Phys* 1989;91:3258.